

# Observation of mutually enhanced collectivity in self-conjugate $^{76}_{38}\text{Sr}$

A. Lemasson,<sup>1</sup> H. Iwasaki,<sup>1,2</sup> C. Morse,<sup>1,2</sup> D. Bazin,<sup>1</sup> T. Baugher,<sup>1,2</sup> J.S. Berryman,<sup>1</sup>  
A. Dewald,<sup>3</sup> C. Fransen,<sup>3</sup> A. Gade,<sup>1,2</sup> S. McDaniel,<sup>1,2</sup> A. Nichols,<sup>4</sup> A. Ratkiewicz,<sup>1,2</sup>  
S. Stroberg,<sup>1,2</sup> P. Voss,<sup>1,2,5</sup> R. Wadsworth,<sup>4</sup> D. Weisshaar,<sup>1</sup> K. Wimmer,<sup>1</sup> and R. Winkler<sup>1</sup>

<sup>1</sup>*National Superconducting Cyclotron Laboratory, Michigan State University, East Lansing, Michigan 48824, USA*

<sup>2</sup>*Department of Physics and Astronomy, Michigan State University, East Lansing, Michigan 48824, USA*

<sup>3</sup>*Institut für Kernphysik der Universität zu Köln, D-50937 Köln, Germany*

<sup>4</sup>*Department of Physics, University of York, Heslington, York YO10 5DD, United Kingdom*

<sup>5</sup>*Simon Fraser University, Burnaby, British Columbia, V5A 1S6 Canada*

(Dated: November 16, 2018)

The lifetimes of the first  $2^+$  states in the neutron-deficient  $^{76,78}\text{Sr}$  isotopes were measured using a unique combination of the  $\gamma$ -ray line-shape method and two-step nucleon exchange reactions at intermediate energies. The transition rates for the  $2^+$  states were determined to be  $B(E2;2^+ \rightarrow 0^+) = 2220(270) \text{ e}^2\text{fm}^4$  for  $^{76}\text{Sr}$  and  $1800(250) \text{ e}^2\text{fm}^4$  for  $^{78}\text{Sr}$ , corresponding to large deformation of  $\beta_2 = 0.45(3)$  for  $^{76}\text{Sr}$  and  $0.40(3)$  for  $^{78}\text{Sr}$ . The present data provide experimental evidence for mutually enhanced collectivity that occurs at  $N = Z = 38$ . The systematic behavior of the excitation energies and  $B(E2)$  values indicates a signature of shape coexistence in  $^{76}\text{Sr}$ , characterizing  $^{76}\text{Sr}$  as one of most deformed nuclei with an unusually reduced  $E(4^+)/E(2^+)$  ratio.

PACS numbers: 21.10.Tg, 23.20.-g, 25.70.-z, 27.50.+e

Deformation of finite quantum systems is a manifestation of spontaneous symmetry breaking. In analogy to the Jahn-Teller effect in molecular physics [1], the coupling between collective vibrations and degenerate excitations of individual nucleons plays an important role in inducing nuclear ground-state deformation [2]. In nuclei, pairing correlations can also compete with the deformation driving particle-vibration coupling, further highlighting rich aspects of this many-body quantum system.

Self-conjugate nuclei have provided challenges to our understanding of the role of deformation driving mechanisms including neutron-proton correlations [3, 4]. In  $N = Z$  nuclei, proton and neutron shell effects can act coherently, promoting an extreme sensitivity of nuclear properties to small changes of nucleon numbers. A well known region is the middle of the  $pf$  shell, where the nuclear shape evolves drastically from triaxial ( $^{64}\text{Ge}$  [5]), to transitional ( $^{68}\text{Se}$  [6]), to oblate ( $^{72}\text{Kr}$  [7]) shapes with a gradual increase of collectivity accompanied by the intrusion of the deformation driving  $g_{9/2}$  orbital [8–10]. This region at  $N = Z$  represents a unique location in the nuclear chart, where a strong enhancement of collectivity is expected from sizable numbers of valence protons and neutrons occupying the same orbitals. However, questions remain to be answered regarding the magnitude and location of – and evolution towards – the maximum collectivity.

In this Rapid Communication, we report on the first measurement of the lifetime of the first  $2^+$  state in the self-conjugate nucleus  $^{76}\text{Sr}$  at  $N = Z = 38$ . We deduce the reduced transition probability  $B(E2;2^+ \rightarrow 0^+)$  (noted  $B(E2\downarrow)$  hereafter). This quantity provides a direct measure of quadrupole collectivity and often serves as a good indicator of the ground-state deformation, particularly

for well-deformed nuclei. A lifetime measurement was also performed for  $^{78}\text{Sr}$  as a reference. Of particular interest are the very low excitation energies  $E(2^+)$  of the first  $2^+$  states measured for  $^{76}\text{Sr}$  [3] and neighboring  $^{78}\text{Sr}$  [3] and  $^{80}\text{Zr}$  [3], which suggest the occurrence of large deformation at  $A \sim 80$  in agreement with theoretical predictions [8–16]. For  $^{76}\text{Sr}$ , the Gamow-Teller strength distribution measured in the  $\beta$ -decay study strongly favors a prolate deformation [17]. Rotational properties of the yrast band are well established in medium and high-spin states up to  $22^+$  in  $^{76}\text{Sr}$  [18]. However, the measured energy ratio  $R_{4/2} = E(4^+)/E(2^+)$  of 2.85 could indicate a triaxial deformation [19] with a reduced collectivity, hampering the establishment of a consistent picture for  $^{76}\text{Sr}$ . Here, based on new  $B(E2\downarrow)$  data, we provide a new perspective on the evolution of collectivity at  $N = Z$  and an insight into the character of the ground-state deformation of  $^{76}\text{Sr}$ .

Exploring deformation of heavy  $N = Z$  nuclei represents an experimental challenge. In this work, the  $\gamma$ -ray line-shape method [20, 21] was applied to measure the lifetimes of the  $2^+$  states of  $^{76,78}\text{Sr}$ , which were produced in two-step nucleon exchange reactions at intermediate energies [22]. A dedicated configuration for the present lifetime measurements was employed for the first time using the Segmented Germanium Array (SeGA) [23] at the National Superconducting Cyclotron Laboratory (NSCL). Also, the present reaction scheme allows access to nuclei that are neutron-deficient but with higher  $Z$  than available primary beams, providing an attractive alternative to the use of fusion evaporation or fragmentation reactions in lifetime measurements. This approach facilitates a clear identification of reaction products and a sizable population of excited states simultaneously.

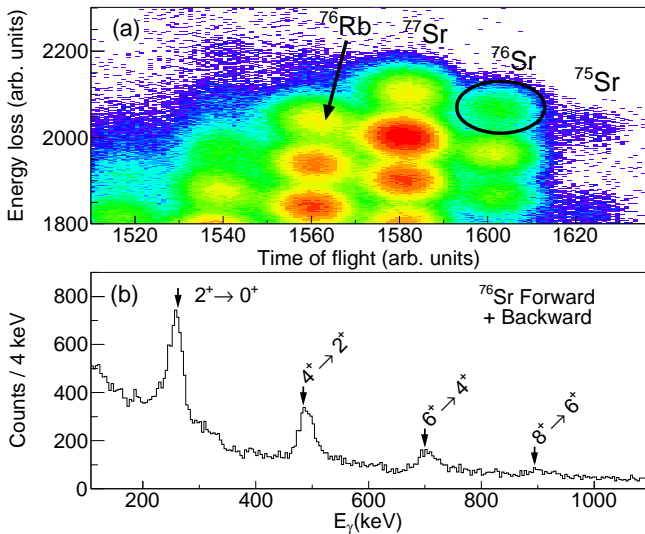


FIG. 1. (color online) (a) Particle identification of reaction residues for the S800 setting optimized for  $^{76}\text{Sr}$ . (b) Doppler-shift corrected  $\gamma$ -ray spectrum for  $^{76}\text{Sr}$  (with  $\beta_{\text{mid}} = 0.396$ ). The arrows indicate the known  $\gamma$ -ray energies [19].

The experiment was performed at the Coupled Cyclotron Facility of NSCL at Michigan State University. Secondary beams of  $^{76}\text{Rb}_{39}$  and  $^{78}\text{Rb}_{41}$  were produced by reactions of a primary beam of  $^{78}\text{Kr}_{42}$  at 140 MeV/nucleon with a  $^9\text{Be}$  target and separated by the A1900 fragment separator [24] using an Al degrader. The momentum acceptance of the A1900 was set to 0.5%. The resultant beams were  $\approx 30\%$   $^{76}\text{Rb}$  at 104.5 MeV/nucleon and  $\approx 70\%$   $^{78}\text{Rb}$  at 101.6 MeV/nucleon for each setting. The available intensity was typically around  $4 \times 10^4$  pps for  $^{76}\text{Rb}$ , while for  $^{78}\text{Rb}$  the beam was used at a rate of  $1 \times 10^5$  pps. The  $^{76}\text{Sr}_{38}$  and  $^{78}\text{Sr}_{40}$  isotopes were produced and studied using the secondary nucleon exchange reactions  $^9\text{Be}(^{76}\text{Rb}, ^{76}\text{Sr}\gamma)\text{X}$  and  $^9\text{Be}(^{78}\text{Rb}, ^{78}\text{Sr}\gamma)\text{X}$ , respectively, on a 376-mg/cm<sup>2</sup>-thick  $^9\text{Be}$  reaction target. The outgoing particles were identified (Fig. 1(a)) based on the time-of-flight and energy-loss measurements using the focal-plane detection system of the S800 spectrometer [25].

De-excitation  $\gamma$  rays were detected by 15 Ge detectors from SeGA [23]. Each Ge crystal has a diameter of 7 cm and is divided into eight 1-cm wide segments along the crystal length. The detectors were arranged around the target in a barrel configuration with the long side of the crystal parallel to the beam axis. Two rings of 7 and 8 detectors were used to cover the forward angles of 50–80° and the backward angles of 95–125°, respectively. The full-energy peak efficiency was measured to be 17.5(3) % at 244 keV by a standard  $^{152}\text{Eu}$  source. The present setup was chosen to maximize  $\gamma$ -ray detection efficiencies as well as the sensitivity to lifetime effects on the  $\gamma$ -ray line-shape as explained later. Figure 1(b) shows an energy

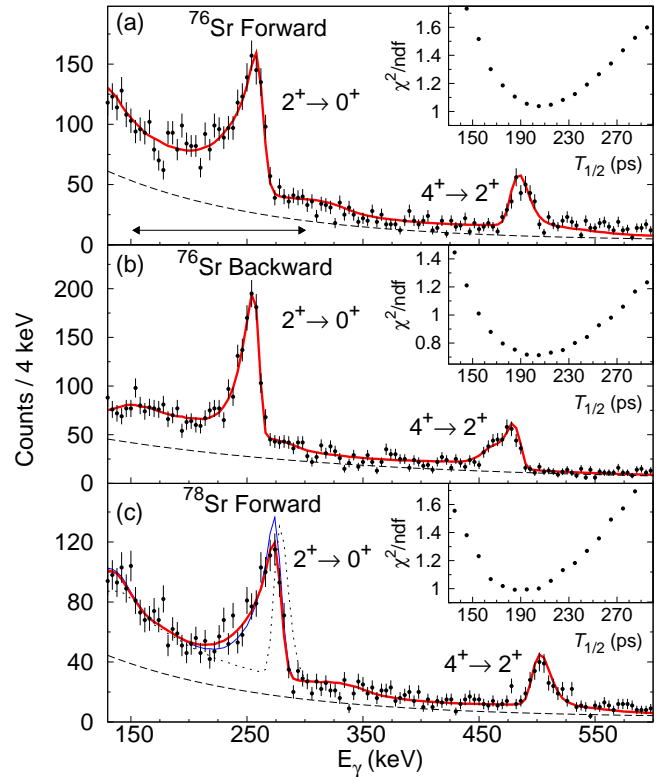


FIG. 2. (color online) Doppler-shift corrected  $\gamma$ -ray spectra obtained for  $^{76}\text{Sr}$  in the (a) forward and (b) backward rings, and (c) for  $^{78}\text{Sr}$  in the forward ring. The data are compared to the simulated spectra (the thick (red) curves) which include background contributions (the dashed curves). The insets show the reduced  $\chi^2$  distributions in the fit. The range of data used in the fit is indicated by the arrow in (a). In (c), the simulated spectra are also shown for the previous data of  $T_{1/2} = 155$  ps [3] (the thin (blue) solid curve) and a reference value of  $T_{1/2} = 0$  ps (the dotted curve).

spectrum of  $\gamma$  rays measured in coincidence with  $^{76}\text{Sr}$ , where the Doppler-shift correction was made by assuming that all  $\gamma$  decays occur in the middle of the target with an average velocity of  $\beta_{\text{mid}} = v/c = 0.396$ . The  $\gamma$ -ray peaks are evident for the yrast band from the  $2^+$  to the  $8^+$  states, demonstrating the ability of the present reaction to populate medium-spin states. Inclusive populations, which are the sum of direct and indirect populations, are estimated to be 51(12)% and 36(8)%, respectively, for the  $2^+$  and  $4^+$  states, showing that about 70% of the  $2^+$  state population was made by feeding from the  $4^+$  state.

In this work, the lifetimes of the  $2^+$  states of  $^{76,78}\text{Sr}$  were determined by the  $\gamma$ -ray line-shape method [20, 21], which is based on the emission-point distribution of  $\gamma$  rays emitted from reaction residues in flight. At the current beam velocities of  $v/c \approx 0.4$ , if an excited-state lifetime is on the order of 100 ps, the  $\gamma$  decay occurs, on average, about 1 cm behind the target. Since we assume the  $\gamma$ -ray decay occurs at the target position to define

the  $\gamma$ -ray emission angles for Doppler-shift corrections, the lifetime effect results in a low-energy tail for a  $\gamma$ -ray peak as well as a slightly lower final peak position. To maximize the sensitivity of the  $\gamma$ -ray line-shape to the lifetime, we produced Doppler-shift corrected spectra of  $^{76,78}\text{Sr}$  by using velocities of outgoing Sr ions measured event-by-event in the S800 (the averaged velocities were  $\beta_{\text{aft}} = 0.335$  for  $^{76}\text{Sr}$  and  $0.330$  for  $^{78}\text{Sr}$ ). As shown in Fig. 2, asymmetric shapes of  $\gamma$ -ray peaks are clearly seen for the  $2^+ \rightarrow 0^+$  transition both in  $^{76}\text{Sr}$  (Figs. 2 (a) and (b)) and  $^{78}\text{Sr}$  (Fig. 2(c)). However, the  $4^+$  peaks are not aligned between the forward and backward data which indicates that the  $4^+$  state decays mostly inside the target with higher recoil velocities. This suggests that the lifetime of the  $4^+$  state is much shorter than the flight time ( $\approx 20$  ps) of the ejectiles passing through the target.

Lifetimes were obtained by comparing the measured spectra to simulated ones as shown in Fig. 2. The simulation is based on an existing code which utilizes GEANT4 [26], with modifications to incorporate the geometry of the present setup. The least  $\chi^2$  method was used in a fitting procedure, where the lifetime of the  $2^+$  state and amplitudes of the simulated spectrum for the  $2^+ \rightarrow 0^+$  transition and an exponential background were taken as variable parameters. The exponential slope of the background was found to be the same for other reaction products and was thus fixed for both  $^{76,78}\text{Sr}$  analyses. The spectral shapes of  $\gamma$  rays depopulating the  $4^+$ ,  $6^+$ , and  $8^+$  states were included in the final fit, where the amplitudes were determined in a different fit. The lifetimes of the  $4^+$  states of  $^{76,78}\text{Sr}$  were both fixed to be equal to that for  $^{78}\text{Sr}$  (half-life  $T_{1/2} = 5.1$  ps) [3]. Based on the reduced  $\chi^2$  distributions as shown in the insets of Fig. 2,  $T_{1/2}$  of the  $2^+$  state in  $^{76}\text{Sr}$  was found to be  $207^{+16}_{-14}$  ps and  $203^{+18}_{-16}$  ps for the forward and backward data, respectively. For  $^{78}\text{Sr}$ ,  $T_{1/2} = 188^{+17}_{-15}$  ps (forward) and  $194^{+21}_{-19}$  ps (backward) were obtained. Systematic errors were mainly due to ambiguities in the geometry of the setup (3%), the feeding from the  $4^+$  state (1%),  $\gamma$ -ray anisotropy effects (1.5%), and the assumption of the background (3%). The overall systematic error in the present measurement was taken to be 4.6% by adding these uncertainties in quadrature.

By combining the forward and backward data, the present results were determined to be  $T_{1/2} = 205(25)$  ps for  $^{76}\text{Sr}$  and  $T_{1/2} = 191(27)$  ps for  $^{78}\text{Sr}$ , where both the statistical and systematic errors are included. The present result for  $^{78}\text{Sr}$  is slightly larger, but consistent with the previous data of  $155(19)$  ps [3]. By adopting  $E(2^+) = 262.3$  keV for  $^{76}\text{Sr}$  [18] and  $277.6$  keV for  $^{78}\text{Sr}$  [27], the  $B(E2\downarrow)$  values are determined to be  $2220(270)$   $\text{e}^2\text{fm}^4$  for  $^{76}\text{Sr}$  and  $1800(250)$   $\text{e}^2\text{fm}^4$  for  $^{78}\text{Sr}$ . Note that main sources of the systematic errors are common for  $^{76,78}\text{Sr}$ , and thus the present results indicate that the collectivity of  $^{76}\text{Sr}$  is larger than that of  $^{78}\text{Sr}$

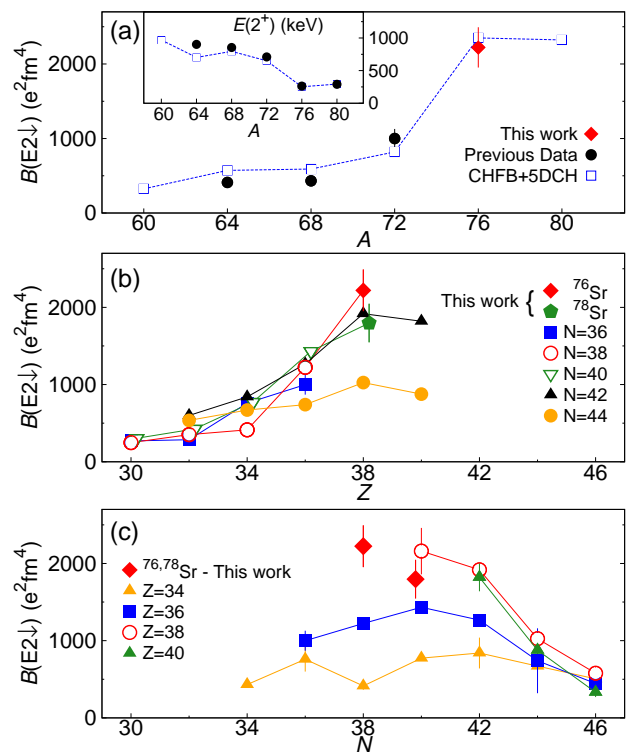


FIG. 3. (color online) (a) Experimental values of  $B(E2\downarrow)$  and  $E(2^+)$  (inset) for the  $N = Z$  nuclei are compared to predictions from the CHFb+5DCH calculations [16]. The  $B(E2\downarrow)$  values in the vicinity of  $^{76}\text{Sr}$  are also plotted in the (b) isotonic and (c) isotopic chains. Data are taken from [3, 5–7, 28, 29].

by about  $2\sigma$ . Following the prescription from Ref. [28] for a rigid rotor, deformation parameters are obtained as  $\beta_2 = 0.45(3)$  for  $^{76}\text{Sr}$  and  $0.40(3)$  for  $^{78}\text{Sr}$ .

The systematic behavior of the  $E(2^+)$  and  $B(E2\downarrow)$  values in the vicinity of  $^{76}\text{Sr}$  are plotted in Fig. 3. Along the  $N = Z$  line, the  $B(E2\downarrow)$  data depict a rapid increase of collectivity from  $^{72}\text{Kr}$  to  $^{76}\text{Sr}$ , accompanied by a sudden decrease in  $E(2^+)$  (Fig. 3(a)). This is consistent with the occurrence of the deformed shell gap at the nucleon number 38 in the Nilsson diagram [8]. However this scheme does not easily account for possible mutual effects of proton and neutron deformation driving contributions at  $N = Z$ . Such effects are studied in Figs. 3 (b) and (c), where the  $B(E2\downarrow)$  data are plotted as a function of  $Z$  ( $N$ ) for the isotonic (isotopic) chain around  $^{76}\text{Sr}$ . In Fig. 3(b), the collectivity increases toward  $Z = 38$  for all the isotonic chains, while the enhancement is largest in the  $N = 38$  chain. For the isotopic chains (Fig. 3(c)), the collectivity is enhanced at  $N = 38$  only when  $Z = 38$ . This observation indicates that the deformed shell gap at the single nucleon number 38 is not strong enough to induce a large ground-state deformation and a mutual support from proton and neutron contributions is essential

for the enhanced collectivity observed for  $^{76}\text{Sr}$ .

From a theoretical point of view, various works [8–16] have attempted to describe the ground-state deformation of nuclei in this region. In Fig. 3(a), the experimental data of  $E(2^+)$  and  $B(E2)$  are compared to the predictions from the constrained-Hartree-Fock-Bogoliubov theory together with a mapping to the five-dimensional collective Hamiltonian (CHFB+5DCH) [16]. Recently, improvements to mean-field theories involving quadrupole correlations [30] and mixing of different deformations [16, 30] have been undertaken to account for the mutually enhanced magicity [31]. A good agreement between the present data and the CHFB+5DCH calculations (Fig. 3(a)) suggests similar improvements are also required to account for the evolution of collectivity around  $^{76}\text{Sr}$ . Particularly, the CHFB+5DCH theory takes into account the mixing of different shapes including a triaxial degree of freedom, reproducing remarkably well the trend and amplitude of the data in the  $A \sim 70$  region [6, 32] with pronounced prolate-oblate shape coexistence. While predictions for spectroscopic information are not available, large deformation for ( $^{76}\text{Sr}$ ,  $^{78}\text{Sr}$ ) are also predicted by other frameworks as (0.37, 0.37) [8], (0.45, 0.45) (RMF with NL-SH interaction [13]), (0.42, 0.42) (FRDM [33]), and (0.44, 0.43) (ETF-SI [34]).

The microscopic origin of the occurrence of the enhanced collectivity in  $A \sim 80$  nuclei is ascribed to the occupation of nucleons in the  $g_{9/2}$  orbital [8–10]. The effect due to the  $g_{9/2}$  intrusion can be clearly seen in the sudden increase of collectivity from  $^{72}_{36}\text{Kr}_{36}$  to  $^{76}_{38}\text{Sr}_{38}$ , where the occupation numbers for the protons and neutrons in the  $g_{9/2}$  orbital are both predicted to increase from about 2 to 3 [9]. Interestingly, the  $g_{9/2}$  occupation of neutrons is predicted to further increase from  $N = 38$  to 40 in the Sr isotopes [9], while the present results show that the maximum collectivity occurs in  $^{76}\text{Sr}$  with  $N = Z = 38$ . This suggests that the deformation driving effects are saturated at the nucleon number of 38 and hence one would expect there to be no additional increase of collectivity in  $^{80}\text{Zr}$ .

To better characterize the collective nature of  $^{76}\text{Sr}$ , a possible signature of shape coexistence phenomena can be investigated based on the systematic behavior for the  $B(E2)$  with respect to the energy ratio  $R_{4/2}$ . If two different configurations coexist, the mixing among them can lead to a reduced  $R_{4/2}$  of the yrast band, as the mixing lowers the ground  $0^+$  state significantly more than other states [35]. In Fig. 4, we plot the correlation between  $R_{4/2}$  and  $B(E2\downarrow)/A$  for the present results of  $^{76,78}\text{Sr}$ . For a systematic comparison, data are also plotted for neighboring Kr ( $Z = 36$ ), Sr ( $Z = 38$ ), and Zr ( $Z = 40$ ) isotopes as well as heavier mid-shell nuclei with  $Z = 62-70$ . As discussed in Ref. [35], the  $B(E2)$  values, when divided by  $A$ , have a clear correlation with  $R_{4/2}$ , starting from vibrational nuclei with  $R_{4/2}$  of 2.0 and evolving to rotational nuclei with  $R_{4/2}$  of 3.3. In fact, the correlation is

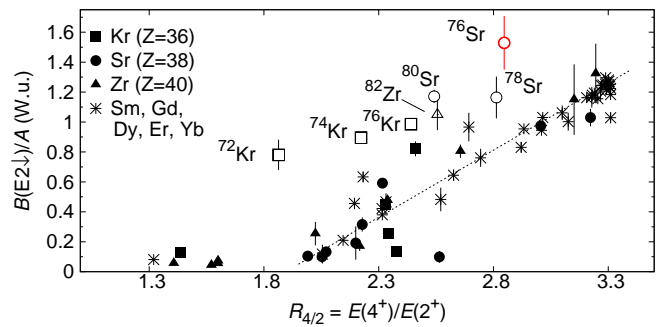


FIG. 4. (color online) Measured  $B(E2)/A$  values against the energy ratios  $R_{4/2} = E(4^+)/E(2^+)$  are plotted for the Kr, Sr, and Zr isotopes around  $Z = 38$  and the  $Z = 62-70$  isotopes (Sm, Gd, Dy, Er, and Yb). Data are taken from Ref. [7, 28, 29] except for  $^{76,78}\text{Sr}$  where present data are shown. The dashed line is to guide the eye.

evident in Fig. 4 for many of the Kr, Sr, and Zr isotopes, shown by the closed symbols, and most of the heavier nuclei. However, the present result for  $^{76}\text{Sr}$ , as well as the  $A = 70 \sim 80$  nuclei highlighted by the open symbols in Fig. 4, significantly deviates from the global behavior, suggesting the signature of shape coexistence. A unique feature for  $^{76}\text{Sr}$  is that the mixing amplitude obtained with a typical mixing strength of 0.2 MeV [36] and a predicted second  $0^+$  state around 1 MeV [10, 16] is very small ( $\sim 5\%$ ), preserving the large ground-state deformation. However, the mixing effect can be amplified in the excitation energy information due to the small  $E(2^+)$ , masking the deformed character of  $^{76}\text{Sr}$  in  $R_{4/2}$ . This emphasizes the importance of the present  $B(E2\downarrow)$  data as a direct indicator of the enhanced collectivity of  $^{76}\text{Sr}$ .

In summary, the present work demonstrated the usefulness of the  $\gamma$ -ray line-shape method combined with two-step nucleon exchange reactions in excited-state lifetime measurements, extending the  $B(E2)$  systematics among self-conjugate nuclei up to  $N = Z = 38$ . The results indicate a large ground-state deformation of  $^{76}\text{Sr}$  with  $\beta_2 = 0.45(3)$  despite the unusually low  $R_{4/2}$  ratio and illustrate the mutual enhancement of collectivity that uniquely occurs at  $N = Z = 38$ . The comparison with theoretical predictions as well as the systematic behaviour of the  $R_{4/2}$  and  $B(E2)$  values highlights the importance of the mixing of coexisting shapes for a rigorous description of well-deformed nuclei in the  $A \sim 80$   $N = Z$  region.

This work is supported by the National Science Foundation under PHY-0606007 and PHY-1102511 and by the UK STFC.

- 
- [1] H. Jahn and E. Teller, *Proc. R. Soc. Lond. A* **161**, 220 (1937).
- [2] A. Bohr, *Rev. Mod. Phys.* **48**, 365 (1976).
- [3] C. Lister *et al.*, *Phys. Rev. Lett.* **49**, 308 (1982).
- [4] A. O. Macchiavelli *et al.*, *Phys. Rev. C* **61**, 041303 (2000); *Phys. Lett. B* **480**, 1 (2000).
- [5] K. Starosta *et al.*, *Phys. Rev. Lett.* **99**, 042503 (2007).
- [6] A. Obertelli *et al.*, *Phys. Rev. C* **80**, 031304(R) (2009).
- [7] A. Gade *et al.*, *Phys. Rev. Lett.* **95**, 022502 (2005).
- [8] W. Nazarewicz *et al.*, *Nucl. Phys. A* **435**, 397 (1985).
- [9] K. Langanke *et al.*, *Nucl. Phys. A* **728**, 109 (2003).
- [10] M. Hasegawa *et al.*, *Phys. Lett. B* **656**, 51 (2007).
- [11] P. Sarriguren, *Phys. Rev. C* **79**, 044315 (2009).
- [12] P. Bonche *et al.*, *Nucl. Phys. A* **443**, 39 (1985).
- [13] G. A. Lalazissis and M. M. Sharma, *Nucl. Phys. A* **586**, 201 (1995).
- [14] A. Petrovici *et al.*, *Nucl. Phys. A* **708**, 190 (2002).
- [15] J. P. Maharana *et al.*, *Phys. Rev. C* **46**, R1163 (1992).
- [16] J. P. Delaroche *et al.*, *Phys. Rev. C* **81**, 014303 (2010), and supplementary material.
- [17] E. Náchter *et al.*, *Phys. Rev. Lett.* **92**, 232501 (2004).
- [18] P. Davies *et al.*, *Phys. Rev. C* **75**, 011302(R) (2007).
- [19] C. Lister *et al.*, *Phys. Rev. C* **42**, R1191 (1990).
- [20] J. R. Terry *et al.*, *Phys. Rev. C* **77**, 014316 (2008).
- [21] P. Doornenbal *et al.*, *Nucl. Instr. and Meth. A* **613**, 218 (2010).
- [22] A. Gade *et al.*, *Phys. Rev. Lett.* **102**, 182502 (2009).
- [23] W. Mueller *et al.*, *Nucl. Instr. and Meth. A* **466**, 492 (2001).
- [24] D. J. Morrissey *et al.*, *Nucl. Instr. and Meth. B* **204**, 90 (2003).
- [25] D. Bazin *et al.*, *Nucl. Instr. Meth. B* **204**, 629 (2003).
- [26] P. Adrich *et al.*, *Nucl. Instr. and Meth. A* **598**, 454 (2009).
- [27] D. Rudolph *et al.*, *Phys. Rev. C* **56**, 98 (1997).
- [28] S. Raman *et al.*, *At. Data Nucl. Data Tables* **78**, 1 (2001).
- [29] A. Gørgen *et al.*, *Eur. Phys. J. A* **26**, 153 (2005).
- [30] M. Bender, G. F. Bertsch, and P.-H. Heenen, *Phys. Rev. C* **73**, 034322 (2006).
- [31] N. Zeldes, T. Dumitrescu, and H. Köhler, *Nucl. Phys. A* **399**, 11 (1983).
- [32] M. Girod *et al.*, *Phys. Lett. B* **676**, 39 (2009).
- [33] P. Möller *et al.*, *At. Data Nucl. Data Tables* **59**, 185 (1995).
- [34] Y. Aboussir *et al.*, *At. Data Nucl. Data Tables* **61**, 127 (1995).
- [35] R. F. Casten and N. V. Zamfir, *Phys. Rev. Lett.* **70**, 402 (1993).
- [36] W. Korten, *Act. Phys. Pol. B* **32**, 729 (2001).